RSC Advances

PAPER

View Article Online
View Journal | View Issue

Cite this: *RSC Adv.*, 2022, **12**, 10051

Development of magnetic molecularly imprinted polymers with double templates for the rapid and selective determination of carbamazepine and lamotrigine in serum†

Ya-qin Wei,‡[a] Lin-lin Zhao,‡[a] Yu-xin You,‡[a] Yan-lin Zhao,[b] Xiao-xiao Zheng,[c] Yan Du[a] and Dao-quan Tang *[acd]

A dual-template magnetic molecularly imprinted polymer (Dt-MMIP) with a specific recognition capability for carbamazepine (CBZ) and lamotrigine (LTG) was synthesized using methacrylic acid as a functional monomer, and ethylene glycol dimethylmethacrylate as a cross-linking agent. A magnetic non-molecularly imprinted polymer without templates (MNIP) was also prepared using the same procedure. The prepared polymers were characterized using scanning electron microscopy, Fourier-transform infrared spectroscopy and adsorption experiments. Results indicated that both Dt-MMIPs and MNIPs were microspherical nanoparticles, and the surface of the Dt-MMIP was rougher than that of the MNIP. In addition, the prepared Dt-MMIPs possessed a higher adsorption capacity and better selectivity for CBZ and LTG than the MNIPs. The maximum static adsorption capacities of Dt-MMIP for CBZ and LTG were 249.5 and 647.9 μg g^{-1}, respectively, whereas those of MNIP were 75.8 and 379.8 μg g^{-1}, respectively. The obtained Dt-MMIPs were applied as a magnetic solid-phase extraction sorbent for the rapid and selective extraction of CBZ and LTG in rat serum samples, and determination was performed by high-performance liquid chromatography with UV detection (HPLC-UV). The developed method of dispersive SPE based on Dt-MMIPs coupled to HPLC-UV has good rapidity and selectivity, and application prospects in serum.

Received 23rd December 2021
Accepted 22nd March 2022

DOI: 10.1039/d1ra09306a

rsc.li/rsc-advances

1. Introduction

As a widely used antiepileptic drug, carbamazepine (CBZ) has been the first-choice antiepileptic drug for a wide range of seizure disorders in both adults and children.[1] CBZ and/or its metabolites including carbamazepine-10,11-epoxide and carbamazepine-10,11-dihydroxide may result in a variety of adverse reactions including immunological, haematological, cutaneous, renal and hepatic disorders.[2] Thus, therapeutic drug monitoring (TDM) is of great importance to clinical analysis and disease treatment, which helps to adjust dosage and achieve an optimal therapeutic effect. Lamotrigine (LTG) can block sodium channels and inhibit glutamate and aspartate release and presents a phenytoin like membrane stabilizing activity.[3] As an anticonvulsant, LTG can be used in nearly all types of described seizures. Although LTG possesses high safety, unpredictable pharmacokinetic interactions with concomitant antiepileptic drugs (AEDs) or other drugs in case of co-therapy, or food may influence the plasma concentration of LTG and then may result in dose-related side effects such as headache, nausea, vomiting, diplopia, dizziness and ataxia.[4] Thus, implementation of TDM is still suggested to meet the needs of individualized treatment of LTG.

TDM of CBZ and LTG mainly includes immunoassay and chromatographic analysis.[5–7] Immunoassays possess simple operation, short feedback times and improved standardization. However, non-specific interference from related compounds, metabolites or a matrix may influence the specificity of immunoassays and thus result in the error of plasma concentration.[8] In the past, chromatographic assays with high selectivity, sensitivity, resolution, precision and accuracy have been widely applied in the individual or simultaneous determination of CBZ or/and LTG in biological samples.[9–14] However, effective and exclusive extraction, separation and enrichment of CBZ and

[a]*Jiangsu Key Laboratory of New Drug Research and Clinical Pharmacy, Xuzhou Medical University, Xuzhou 221004, China*

[b]*Department of Pharmacy, Suining People's Hospital Affiliated to Xuzhou Medical University, Suining 221202, China*

[c]*Department of Pharmacy, Xuzhou Municipal Hospital Affiliated to Xuzhou Medical University, Xuzhou 221002, China*

[d]*Department of Pharmaceutical Analysis, Xuzhou Medical University, 209 Tongshan Road, Xuzhou 221204, Jiangsu Province, China. E-mail: tdq993@hotmail.com; tangdq@xzhmu.edu.cn; Fax: +86 516 83263133; Tel: +86 516 83263133*

† Electronic supplementary information (ESI) available. See DOI: 10.1039/d1ra09306a

‡ These authors contributed to the work equally and should be regarded as co-first authors.

LTG in biological matrix are still a key topic in chromatographic analysis. Except for conventional protein precipitation using methanol, acetonitrile or acetone as precipitant, solid phase extraction, especially based on molecularly imprinted polymers (MIPs), has attracted more attentions.[15–20] Except for the application of MIPs in pharmaceutical fields of removal of genotoxic impurity in active pharmaceutical ingredient,[21] and drug delivery,[22] SPE used magnetic MIPs (MMIPs) as adsorbents is a new biological sample pre-treatment method, which need not to be packed MMIPs into an SPE cartridge and presents the advantages of both high selectivity of MIPs and easy separation of magnetic separation. Thus, SPE based on MMIPs has attracted considerable attention as a pre-treatment method for LTG or CBZ biological samples.[16,19]

Accordingly, this study prepared a double-template magnetic MIPs (Dt-MMIPs) on the surface of magnetic silica nanoparticles (Fe_3O_4@SiO_2) by using CBZ and LTG as template molecules. Firstly, Fe_3O_4@SiO_2 was prepared through co-precipitation and tetraethoxysilane (TEOS) hydrolysis under an alkaline medium at 40 °C. Subsequently, 3-methacryloxypropyltrimethoxysilane (MPTS) were modified onto the surface of Fe_3O_4@SiO_2 at 120 °C to obtain Fe_3O_4@SiO_2@MPTS. Finally, the Dt-MMIP was prepared by copolymerization of Fe_3O_4@SiO_2@MPTS with the preassembled solution of templates and the monomer methacrylic acid (MAA), the cross-linking agent ethyleneglycol dimethacrylate (EGDMA) and the initiator 2,2-azobisisobutyronitrile (AIBN). The prepared Dt-MMIPs were characterized by Fourier-transform infrared (FTIR) spectroscopy, scanning electron microscopy (SEM) as well as static, dynamic and selective adsorption experiments. Coupled to high performance liquid phase with ultraviolet detector (HPLC-UV) analysis, the obtained Dt-MMIP was applied as a magnetic SPE sorbent to extract CBZ and LTG in rat serum. The analytical performance and applied ability were also evaluated by comparing with conventional acetonitrile protein precipitation.

2. Materials and methods

2.1. Materials and reagents

Chromatographic grade acetonitrile (≥99.9%) and methanol (≥99.9%) were obtained from Fisher (Pittsburgh, PA, USA). Analytical grade toluene (≥99.5%) and dichloromethane (≥99.5%) were purchased from Sinopharm Chemical Reagent Co. Ltd. (Shanghai China). Analytical grade ferrous chloride tetrahydrate ($FeCl_2 \cdot 4H_2O$) (99.0%), ferric trichloride hexahydrate ($FeCl_3 \cdot 6H_2O$) (98.0%), tetramethylsilane (TEOS) (98.0%), ammonium hydroxide (25.0–28.0%), azobisisobutyronitrile (AIBN) (98.0%), 3-methacryloxypropyltrimethoxysilane (MPTS) (97.0%), 4-vinyl benzoic acid (4-VBA) (97.0%), 4-vinyl pyridine (4-VP) (95.0%), divinylbenzene (DVB) (80%), and trimethylpropane trimethacrylate (TRIM) (98.0%) were obtained from Energy Chemical (Shanghai, China). Methacrylic acid (MAA) (99%) and ethylene glycol dimethacrylate (EGDMA) (98%) were purchased from Aladdin Biochemical Technology Co., Ltd. (Shanghai, China). Distilled water was purchased from Guangzhou Watson's Food & Beverage Co., Ltd. (Guangzhou, China). The standard references including CBZ (99.0%), LTG (≥98.0%), oxcarbazepine (OXC) (≥98.0%), phenobarbital (PB) (≥98.0%), phenytoin (PHT) (≥98.0%), primidone (PRM) (≥98.0%), and benzoguanamine (BGA) (≥98.0%) were purchased from the National Institute for the Control of Pharmaceutical and Biological Products (Beijing, China) and their chemical structures were shown in Fig. S1.†

2.2. Dt-MMIP preparation

As showed in Fig. 1, first, Fe_3O_4 nanoparticle were synthesized *via* chemical co-precipitation according to our and other's previous work with some modifications.[23,24] $FeCl_3 \cdot 6H_2O$ (10.8 g) and $FeCl_2 \cdot 4H_2O$ (3.9 g) were dissolved in 100 mL of distilled water and then heated under a nitrogen atmosphere and stirred mechanically. When the reaction temperature reached 70 °C, 10 mL of ammonium hydroxide solution (25%) was immediately added into the solution. After reacting at 80 °C for 30 min, 0.4 g of sodium citrate was then added as dispersant. After holding at 80 °C for 30 min and the reaction solution was then naturally cooled to room temperature. The obtained black precipitate was separated with a permanent magnet and then washed several times successively with ethanol and distilled water. The products were dried in a vacuum oven at 60 °C for 12 h.

Next, 360 mL of ethanol, 20 mL of ammonium hydroxide solution (25%), 90 mL of distilled water, 10 mL of TEOS and approximately 13 g of the synthesized Fe_3O_4 nanoparticles were mixed and reacted *via* mechanical stirring at 400 rpm and 40 °C water bath for 12 h. The black precipitate (Fe_3O_4@SiO_2) was isolated with a magnet, washed with ethanol and distilled water for several times, and then dried under vacuum at 60 °C for 12 h.

Subsequently, 0.5 g of Fe_3O_4@SiO_2, 50 mL of toluene and 5 mL of MPTS were mixed and reacted under a nitrogen atmosphere *via* mechanical stirring at 400 rpm and 120 °C oil bath for 24 h. The precipitate (Fe_3O_4@SiO_2@MPTS) was isolated

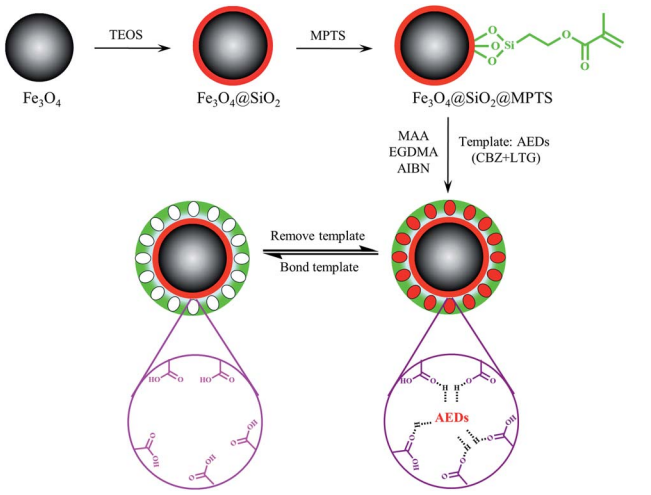

Fig. 1 Schematic illustration of the preparation procedure of double-template magnetic molecularly imprinted polymers (Dt-MMIPs).

with a magnet, washed with ethanol and distilled water for several times, and then dried under vacuum at 60 °C for 12 h.

Finally, 425 μL (5 mmol) of MAA as added in 60 mL of methanol–acetonitrile (1 : 1, v/v) and then added 118 mg (0.5 mmol) of CBZ and 128 mg (0.5 mmol) of LTG. After ultrasonic treatment for 30 min, the reaction solution was stood at 4 °C for 12 h. Then, 0.5 g of Fe_3O_4@SiO_2@MPTS, 50 mg of AIBN and 6.98 mL (35 mmol) of EGDMA were added in this preassemble solution and ultrasonically treated for 15 min. After N_2 was introduced for 40 min, the reaction solution was sealed and then reacted *via* mechanical stirring at 400 rpm and 60 °C water bath for 24 h. The gray product was isolated using a magnet and washed with methanol and distilled water for several times. The templates were then removed successively by Soxhlet extraction using methanol–glacial acetic acid (9 : 1, v/v) until no CBZ or LTG was detected by the HPLC-UV. The magnetic particles were dried at 60 °C for 12 h and denoted as Dt-MMIPs. Similarly, a magnetic non-imprinted polymer (MNIP) for comparison was simultaneously prepared under the same procedure without the templates.

2.3. Characterization of MIPs

A FTIR-8400S Fourier transform infrared spectroscopy system (Shimadzu, Japan) was used to characterize polymers. The surface morphology and structures of the materials including Fe_3O_4@SiO_2, Fe_3O_4@SiO_2@MPTS, Dt-MMIPs and MNIPs were identified using a FEI Quanta 450FEG SEM system (Hillsboro, USA).

2.4. HPLC analysis

HPLC analysis was carried out using a Water e2695 Alliance HPLC System (Massachusetts, USA). Chromatographic separation of CBZ, LTG, OXC, PHB, PHT, PRM, or BGA was all performed on an Agilent Zorbax Eclipse Plus C18 column (4.6 mm × 100 mm, 3.5 μm) with a gradient acetonitrile (A) and water (B) at a flow rate of 1 mL min^{-1}. The elution procedures were set as follows: 0–9 min, 10% B–55% B; 9–11 min, 55% B–10% B; 11–15 min, 10% B. The column temperature was maintained at 30 °C and the injection volume was 20 μL. The detection wavelengths of CBZ, LTG, OXC, PHB, PHT, PRM and BGA were set at 285 nm, 307 nm, 306 nm, 230 nm, 240 nm, 215 nm and 245 nm, respectively.

2.5. Adsorption test

The static adsorption test was performed as follows: 60 mg of Dt-MMIPs were dispersed in 5 mL of the mixed solution containing CBZ and LTG at different concentrations (1, 3, 5, 10, 15 and 20 μg mL^{-1}) in a centrifuge tube (10 mL). The mixture was shaken for 1 h in an incubator shaker controlled at 300 rpm and 30 °C and then separated with a magnet. Subsequently, the supernatant was filtered with a 0.22 μm organic filter membranes and measured with HPLC-UV.

The data of static adsorption for the uptake of CBZ and LTG on the Dt-MMIP were further fitted to the Langmuir, Freundlich and Dubinin–Radushkevich isothermal equations in the linearized form, which were respectively expressed as:

$$\frac{C_e}{q_e} = \frac{K}{q_m} + \frac{C_e}{q_m} \quad (1)$$

$$\ln q_e = \frac{1}{n} \ln C_e + \ln K_F \quad (2)$$

$$\ln q_e = \ln q_m - \beta\varepsilon^2 \quad (3)$$

where q_e was the equilibrium adsorption amount (μg g^{-1}), C_e was the equilibrium concentration in the solution (μg mL^{-1}), q_m represented the maximum amount of CBZ or LTG that could be adsorbed on the Dt-MMIP (μg g^{-1}), K was the constant of Langmuir model (μg mL^{-1}), K_F (μg g^{-1}) and n were the Freundlich constants depicting the adsorption process, ε was the Polanyi potential ($\varepsilon = RT\ln(1 + 1/C_e)$), β was the activity coefficient associated with adsorption free energy ($mol^2\ J^{-2}$), T was the absolute temperature and R was the gas constant (8.314 J mol^{-1} K^{-1}).

The dynamic adsorption test was carried out in a similar manner, except that the amount of Dt-MMIPs was set at 60 mg. The measurements were obtained at different times (2, 5, 10, 15, 20, 30, 40, 60, 90 and 120 min). According to the concentration difference of CBZ or LTG before and after adsorption by Dt-MMIPs, the adsorption capacity (Q_e, μg g^{-1}) was calculated using the following equation:

$$Q_e = \frac{(C_0 - C_e)V}{W} \quad (4)$$

where C_0 (μg mL^{-1}) is the initial concentration of CBZ or LTG solution, C_e (μg mL^{-1}) is the concentration of CBZ or LTG in the supernatant solution after the adsorption equilibrium, V (mL) is the volume of the solution and W (g) is the dry weight of Dt-MMIPs.

To further study the adsorption kinetic mechanism, the pseudo-first-order rate (eqn (5)) and pseudo-second-order rate (eqn (6)) were respectively applied to fit the kinetic data and calculated using the following equation:

$$\ln(Q_e - Q_t) = \ln Q_e - \frac{k_1 t}{2.303} \quad (5)$$

$$\frac{t}{Q_t} = \frac{1}{k_2 Q_e^2} + \frac{t}{Q_e} \quad (6)$$

where Q_e and Q_t (μg g^{-1}) are the adsorption capacity of LTG or CBZ adsorbed on the Dt-MMIPs at equilibrium and at time t (min), respectively. k_1 (1/min) and k_2 (μg min g^{-1}) are the corresponding adsorption rate constants of pseudo-first-order and pseudo-second-order, respectively.

2.6. Desorption test

Desorption experiment was carried out as follows: a batch of 60 mg of Dt-MMIPs was added into 5 mL of mixed standard solution (concentration of LTZ or CBZ was all 10 μg mL^{-1}). The mixtures were continuously shaken for 1 h at 30 °C to ensure the adsorption was complete. Then, the analytes adsorbed onto the Dt-MMIPs were eluted by 5.0 mL of methanol by shaking at room temperature for 1 h, and the recoveries of the analytes was

calculated by the ratio of the concentrations of analytes in elution detected by HPLC-UV with their initial concentrations.

2.7. Selective adsorption test

The selective adsorption capacity of the Dt-MMIPs and was MNIPs towards on LTG and CBZ evaluated using OXC, OXC, PHB, PHT, PRM and BGA as interferences. Approximately 60 mg of Dt-MMIPs or MNIPs were added to a centrifuge tube (10 mL) containing a 5 mL of mixed standard solution of LTG and CBZ (concentration of LTG or CBZ all was 10 μg mL^{-1}). The mixtures were shaken for 30 min at 30 °C and 300 rpm and then separated using a magnet. The supernatant was filtered through a 0.22 μm organic filter membrane and then determined by HPLC-UV. The interferences were performed as the same manner. The distribution coefficient (K_d) and selection coefficient (K_s) were calculated using the following equation:

$$K_d = \frac{Q_e}{C_e} \quad (7)$$

$$K_s = \frac{K_{d(\text{template})}}{K_{d(\text{interferent})}} \quad (8)$$

where K_d (mL g^{-1}) is the distribution coefficient, C_e (μg mL^{-1}) is the concentration in the supernatant solution after the adsorption equilibrium, Q_e (μg g^{-1}) is the equilibrium adsorption capacity calculated by the eqn (1), and K_s is the selectivity coefficient.

The relative selectivity coefficient (K_{rs}) used to estimate the effect of imprinting on selectivity was calculated using the following equation:

$$K_{rs} = \frac{K_{s(\text{Dt-MMIP})}}{K_{s(\text{MNIP})}} \quad (9)$$

where $K_{s(\text{Dt-MMIP})}$ and $K_{s(\text{MNIP})}$ are the selectivity coefficients of the prepared Dt-MMIPs and MNIPs, respectively. The larger the value of K_{rs}, the better the adsorption affinity and selectivity of the magnetic imprinting material for the template as compared with the non-imprinting material.

2.8. Application evaluation in the determination of serum

2.8.1. Sample treatment. 200 μL of serum was added in 200 μL of phosphate buffer solution (pH 7.0) and mixed evenly. Then, 20 mg of Dt-MMIPs was added in this mixture and shaken for 1 h in an incubator shaker controlled at 300 rpm and 30 °C. After separating with a magnet and then washing with distilled water, the Dt-MMIPs were eluted with 2 mL of methanol by shaking at room temperature for 1 h. After separating with a magnet, the supernatant was evaporated to dryness in a thermostatic water bath at 40 °C under a gentle stream of nitrogen. The residue was re-dissolved with 100 μL of 70% acetonitrile aqueous solution and centrifuged at 4 °C 12 000 rpm for 15 min. The supernatant was filtered through a 0.22 μm organic filter membrane and then determined by HPLC-UV.

For comparison, serum protein precipitation using acetonitrile was also performed. Simply, 200 μL of serum was added in 600 μL of acetonitrile and then whirled together by a vortexer for 30 s. The mixture was then centrifuged at 12 000 rpm and 4 °C for 10 min. The supernatant was evaporated to dryness in a thermostatic water bath at 40 °C under a gentle stream of nitrogen. The residue was re-dissolved with 100 μL of 70% acetonitrile aqueous solution and centrifuged at 4 °C 12 000 rpm for 15 min. The supernatant was filtered through a 0.22 μm organic filter membrane and then determined by HPLC-UV.

Here, the evaporation and re-dissolution was to meet the requirement of comparison. In practical work, these steps could be omitted.

2.8.2. Application evaluation. Calibration standards and quality control (QC) samples prepared by spiking blank rat serum with CBZ and LTG were used to evaluate the analytical performances of dispersive SPE based on Dt-MMIPs coupled with HPLC-UV from aspects of matrix interference, linearity and ranges, accuracy and precision, stability and extraction recovery. Real rat serum was used to evaluate the application ability of developed Dt-MMIPs/HPLC-UV. All animal procedures were performed in accordance with the Guidelines for Care and Use of Laboratory Animals of Xuzhou Medical University and approved by the Animal Ethics Committee of Xuzhou Medical University (No. 201902A031). As a comparison, those experiments were simultaneously performed by conventional protein precipitation using acetonitrile.

3. Results and discussion

3.1. Preparation of the Dt-MMIPs

Dt-MMIPs were prepared using different types of functional monomers including MAA, VBA and 4-VP under the conditions of the constant amounts of functional monomer, templates, cross-linking agent EGDMA, initiator AIBN, porogen methanol–acetonitrile (1 : 1, v/v) and Fe_3O_4@SiO_2@MPTS, and the adsorption capacity (Q_e) of synthesized Dt-MMIPs towards on templates was calculated according to the eqn (1) and evaluated. As shown in Fig. S2A,† MAA was the best choice as functional monomer in this work. Subsequently, the amount of MAA was further optimized as the same manner. As depicted in Fig. S2B,† the best molar ratio of MAA to total amount of LTG and CBZ was 1 : 5.

Different types of cross-linking agents including DVB, EGDMA and TRIM, and porogens including methanol, methanol–acetonitrile (1 : 1, v/v) and dichloromethane, and the amount of EGDMA, methanol–acetonitrile (1 : 1, v/v), AIBN and Fe_3O_4@SiO_2@MPTS were optimized as the same manners with functional monomer. As shown in Fig. S2C–H,† the best molar ratio of EGDMA to the total amounts of LTG and CBZ, and the amounts of methanol–acetonitrile (1 : 1, v/v), AIBN and Fe_3O_4@SiO_2@MPTS were 1 : 35, 40 mL, 50 mg and 0.6 g.

3.2. Characterization of Dt-MMIPs and MNIPs

FT-IR analysis was shown in Fig. 2. Strengthened peaks at 1720 cm^{-1} (C=O stretching) indicated the presence of carboxylic groups in MAA influenced by EGDMA. Peaks near 1100 cm^{-1} corresponded to the Si–O–Si stretching vibration, which

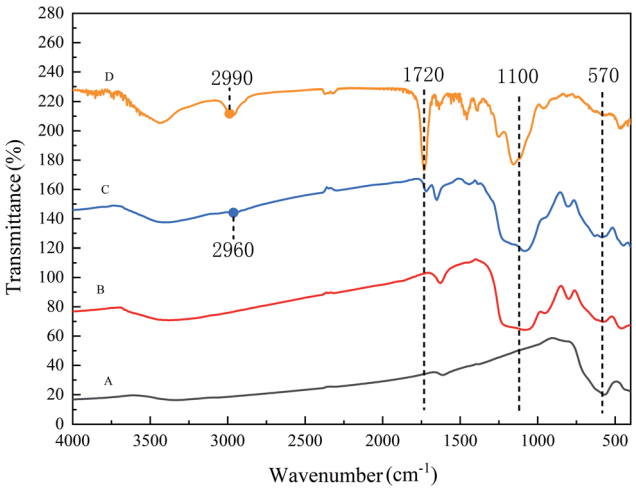

Fig. 2 FT-IR spectra of Fe_3O_4 (A), Fe_3O_4@SiO_2 (B), Fe_3O_4@SiO_2@MPTS (C) and Dt-MMIPs (D).

suggested the existence of the SiO_2 layer. Peak at 2960 cm^{-1} (C–H stretching) indicated the presence of methyl groups, while peak at 2990 cm^{-1} hinted the presence of unsaturated C–H stretching from EGDMA. Peaks near 570 cm^{-1} (Fe–O stretching) verified the encapsulation of Fe_3O_4 into the Dt-MMIPs.

The morphology of the polymers characterized by SEM illustrated that the Fe_3O_4 nanoparticles possessed a smooth surface and regular morphology with a particle size of 100–280 nm (Fig. 3A). After silanization and modified with MPTS (Fig. 3B), the sphericity of Fe_3O_4@SiO_2@MPTS remained good, and the particle size distribution was relatively uniform and gradually increased. However, MPTS modification made the dispersibility increasing slightly and the surface rough. As shown in Fig. 3C and D, compared with MNIPs, Dt-MMIPs had a rougher surface, which might be caused by the surface pore structure and the appearance of imprinted cavities after removing of templates.

3.3. Adsorption performance for CBZ and LTG

3.3.1. Static adsorption. The static adsorption test was performed by calculating the adsorption capacities of Dt-MMIPs and MNIPs towards on CBZ and LTG at different concentrations under the same condition, and the adsorption isotherm was mapped in Fig. 4. As shown in Fig. 4, the amount of CBZ or LTG bounding to Dt-MMIPs or MNIPs increased with the increasing of CBZ and LTG concentrations and then flattened after adsorption saturation. The adsorption capacities of Dt-MMIPs for CBZ or LTG reached respectively 249.5 μg g^{-1} and 647.9 μg g^{-1}, which was higher than that bound to the MNIPs (75.8 μg g^{-1} for CBZ and 379.8 μg g^{-1} for LTG). Those results hinted that Dt-MMIPs possessed good imprinting effect for CBZ or LTG, and might be suitable for the enrichment of CBZ and LTG in biological samples.

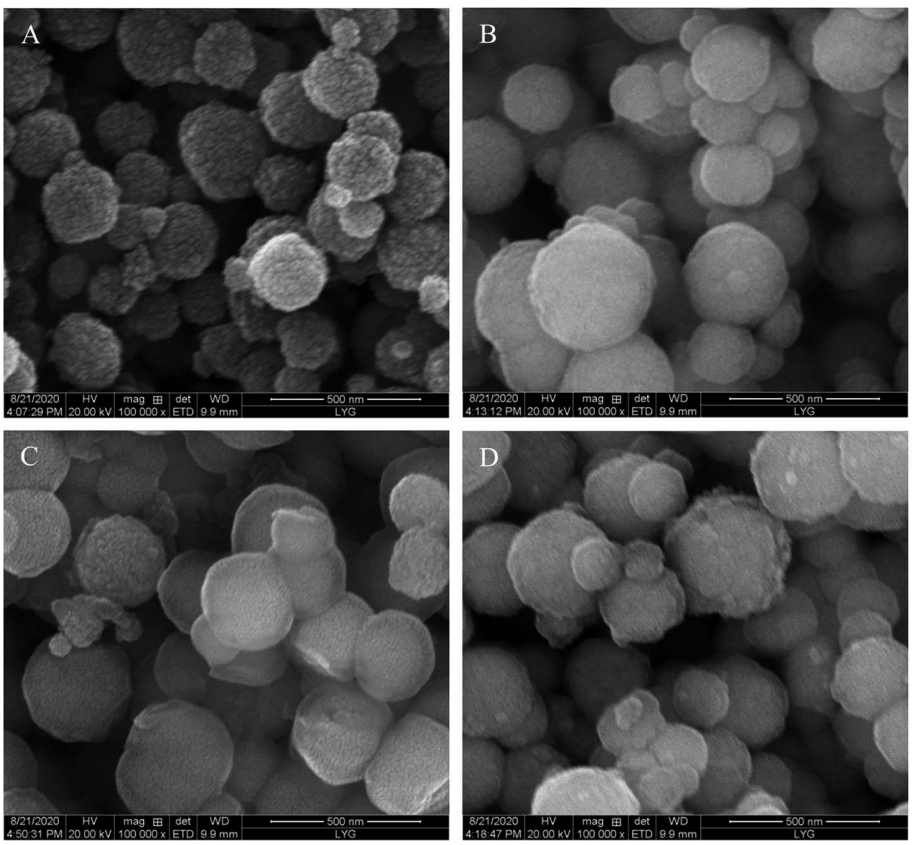

Fig. 3 SEM photographs of Fe_3O_4 (A), Fe_3O_4@SiO_2@MPTS (B), Dt-MMIPs (C) and MNIPs (D).

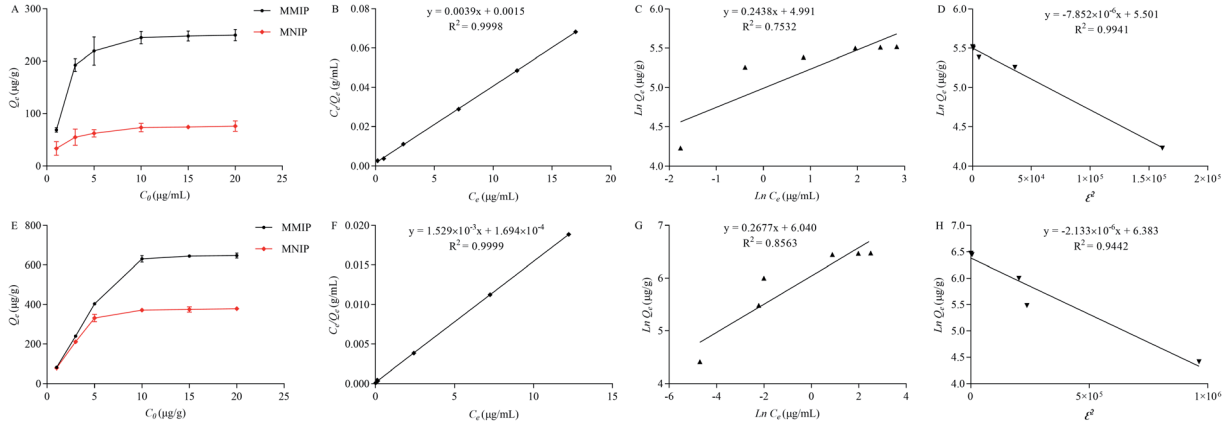

Fig. 4 The adsorption isotherm curves of Dt-MMIPs and MNIPs for CBZ (A) and LTG (E) ($n = 3$) and illustration of the isotherm data presented in terms of the linearized Langmuir (B or F), Freundlich (C or G) and Dubinin–Radushkevich (D or H) models.

The Langmuir model assumed that there were not interactions between adsorbed molecules and no transmigration of adsorbed molecules on the adsorption surface and the monolayer adsorption occurred at binding sites with homogeneous energy levels. The Freundlich model hypothesized the exponential distribution of adsorption sites and multilayer adsorption. The Dubinin–Radushkevich model presented the adsorption process through Gaussian energy distribution on a heterogeneous surface. The linear plots of the Langmuir, Freundlich and Dubinin–Radushkevich equations were shown in Fig. 4 and the constants of the above equations including correlation coefficients were summarized in Table 1. As shown in Fig. 4 and Table 1, the adsorption of CBZ and LTG was well fitted to the Langmuir model with the higher R^2 value (0.9998 or 0.9999), which indicated that the adsorption between CBZ or LTG and Dt-MMIP occurred at specific homogeneous sites within the adsorbent to form monolayer coverage of CBZ or LTG at the surface of the absorbent.

A dimensionless constant separation factor (R_L) could be used to predict the essential characteristics and the feasibility of the Langmuir model and calculated as:

$$R_L = 1/(1 + KC_0) \quad (10)$$

where K was the Langmuir isotherm constant and C_0 was the initial concentration of CBZ or LTG (μg mL^{-1}). The value of R_L indicated the shape of the isotherm to be either unfavorable ($R_L > 1$), linear ($R_L = 1$), favorable ($0 < R_L < 1$) or irreversible ($R_L = 0$). In our current study, the R_L values for the adsorption of CBZ and LTG on the Dt-MMIP were in the ranges of 0.115–0.722 or 0.273–0.882, respectively, which indicated that the adsorption of CBZ and LTG on the Dt-MMIP presented a favorable process.

3.3.2. Dynamic adsorption. The adsorption kinetics that defines the efficiency of adsorption is an important factor for Dt-MMIPs. Fig. 5 presented the adsorption kinetics of Dt-MMIPs towards on CBZ and LTG including the plots of the experimental data and the model fitting. As shown in Fig. 5, under the fixed templates concentration, the adsorption amounts of Dt-MMIPs towards on CBZ or LTG rapidly increased during the first 30 min or 10 min, respectively, and then gradually flattened. The adsorption equilibrium of CBZ and LTG could be reached approximately within 40 min or 30 min, respectively. A good correlation for the adsorption of CBZ and LTG on Dt-MMIPs could be obtained in the pseudo-second-order kinetic model. Table 2 listed the adsorption kinetic constants and linear regression values. Compared with the pseudo-first-order model, the correlation coefficient (R^2) of the pseudo-second-order model was better, and the Q_e parameters of the pseudo-second-order model were closer to the experimental values. Those results suggested that the chemical interactions might involve in the adsorption process and the adsorption rate might be controlled by the movement of template molecules within the pore of Dt-MMIPs.

3.4. Adsorption selectivity

To investigate the adsorption selectivity of Dt-MMIPs for CBZ and LTG, the structural analogues of CBZ including OXC and PHT or that of LTG including PHB, PRM and BGA were selected for selectivity test, respectively. As depicted in Table 3 and Fig. 6,

Table 1 Parameters of Langmuir, Freundlich and Dubinin–Radushkevich isothermal equations for adsorption of CBZ and LTG on the Dt-MMIP

	Langmuir			Freundlich			Dubinin–Radushkevich		
Substrate	q_m (μg g^{-1})	K (μg mL^{-1})	R^2	n	K_F (μg g^{-1})	R^2	q_m (μg g^{-1})	ε (mol^2 J^{-2})	R^2
CBZ	256.4	0.3846	0.9998	4.102	147.0	0.7532	244.9	0.000008	0.9941
LTG	666.7	0.1333	0.9999	3.736	420.0	0.8563	591.5	0.000002	0.9442

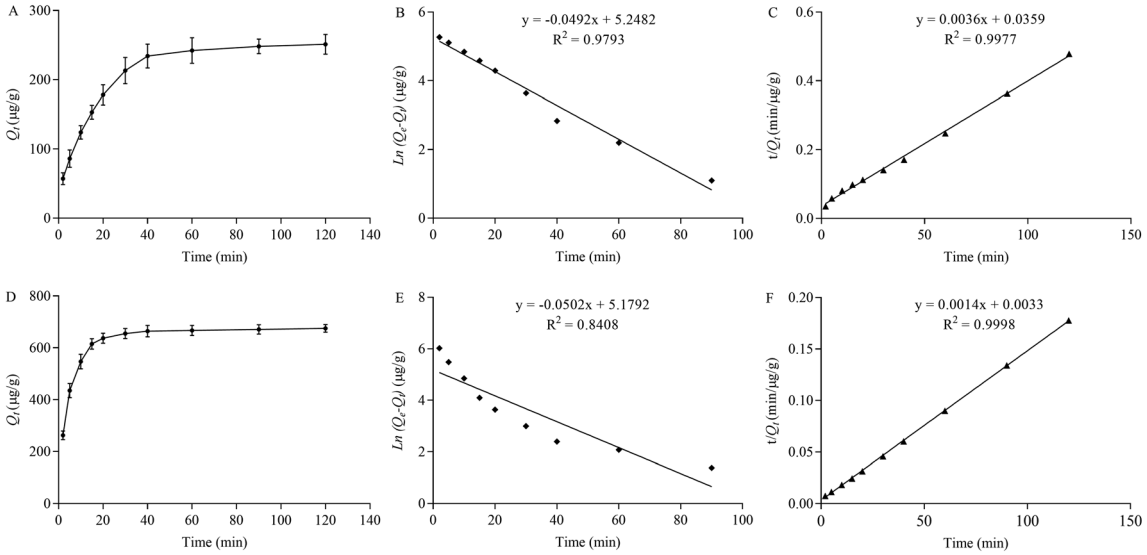

Fig. 5 The dynamic adsorption plots (A or D) ($n = 3$), pseudo-first-order (B and E) and pseudo-second-order (C and F) kinetic models for the adsorption of CBZ and LTG by Dt-MMIPs.

Table 2 Kinetics constants for adsorption of CBZ and LTG on the Dt-MMIP

		Pseudo-first-order kinetic model			Pseudo-second-order kinetic model		
Substrate	$Q_{e(exp)}$ (μg g^{-1})	$Q_{e(cal)}$ (μg g^{-1})	k_1	R^2	$Q_{e(cal)}$ (μg g^{-1})	k_2	R^2
CBZ	251.2	190.2	0.0492	0.9793	277.8	0.000361	0.9977
LTG	675.3	177.5	0.0502	0.8408	714.3	0.000594	0.9998

Table 3 Adsorptive selectivity of Dt-MMIP and MNIP towards on CBZ and LTG

	Dt-MMIPs					MNIPs							
Substrate	Q_e (μg g^{-1})	K_d (mL g^{-1})	$K_{s(OXC)}$	$K_{s(PHT)}$		Q_e (μg g^{-1})	K_d (mL g^{-1})	$K_{s(OXC)}$	$K_{s(PHT)}$		$K_{rs\ (OXC)}$	$K_{rs\ (PHT)}$	
CBZ	244.0	34.5	0.9	3.6		71.0	7.8	0.5	1.2		1.9	3.0	
OXC	263.0	38.5	—	—		138.4	16.6	—	—				
PHT	84.8	9.5	—	—		59.0	6.3	—	—				
Substrate	Dt-MMIPs					MNIPs					$K_{rs(BGA)}$	$K_{rs(PHB)}$	$K_{rs(PRM)}$
	Q_e (μg g^{-1})	K_d (mL g^{-1})	$K_{s\ (BGA)}$	$K_{s(PHB)}$	$K_{s(PRM)}$	Q_e (μg g^{-1})	K_d (mL g^{-1})	$K_{s(BGA)}$	$K_{s(PHB)}$	$K_{s(PRM)}$			
LTG	657.7	312.0	13.6	24.3	20.4	376.7	68.7	6.6	7.1	6.8	2.0	3.4	3.0
BGA	179.8	22.9	—	—	—	92.0	10.3	—	—	—			
PHB	111.0	12.8	—	—	—	86.8	9.7	—	—	—			
PRM	129.3	15.3	—	—	—	90.6	10.2	—	—	—			

Dt-MMIPs had significantly higher adsorption capacity for CBZ than PHT, but has no obvious difference between CBZ and OXC. This result might be attributed to the high similarity of OXC (CBZ-10,11-epoxide) structural and molecular size with CBZ, which also was the basis of dummy template applied in the preparation of MIPs.[25] For LTG, its adsorption capacity on Dt-MMIPs was significantly higher than that of BGA, PHB and PRM. Furthermore, the absorption capacity of LTG on Dt-MMIPs was significantly higher than that of CBZ and OXC. These results indicated that the synthesized Dt-MMIPs has higher molecular recognition selectivity to CBZ or LTG than their relative structural analogues except OXC, and the molecular recognition selectivity of Dt-MMIPs towards on LTG was higher than that CBZ. Compared with Dt-MMIPs, the MNIPs offered lower adsorption capacities for CBZ, LTG and the interferences, which might result from the absence of proper cavities and recognition sites in MNIPs. Moreover, MNIPs provided higher adsorption capacities of OXC or LTG than that of CBZ and PHT, or than that of BGA, PHB and PRM, which might result from the special active groups existed on OXC or LTG that could be bounded to MIPs. Analysis from the values of K_d, K_s and K_{rs} further clarified the above results, and the K_{rs}

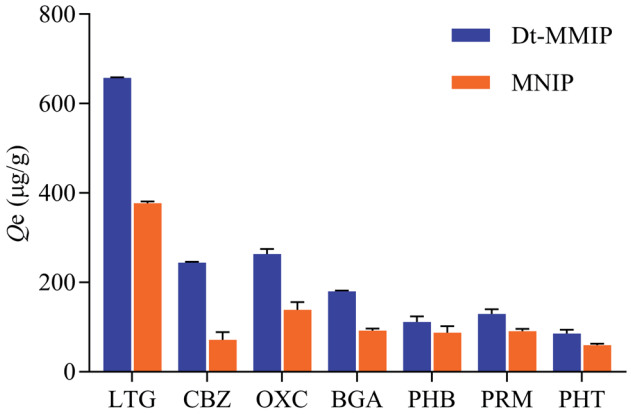

Fig. 6 Absorption selectivity plots of Dt-MMIP and MNIP towards on LTG, CBZ, OXC, BGA, PHB, PRM and PHT.

values of Dt-MMIPs for CBZ/OXC, CBZ/PHT, LTG/BGA, LTG/PHB and LTG/PRM were 1.9-, 3.0-, 2.0-, 3.4- and 3.0-fold higher than those of MNIPs, respectively. These results also confirm that the recognition ability of Dt-MMIPs was better for the templates than for the non-templates. Therefore, the double-template imprinting mode increased the adsorption capacity, and competitive and selective ability of the polymer.

3.5. Optimization of desorption parameters

The types of desorption reagents including methanol, ethanol and distilled water, and desorption times at 1, 5, 10, 30, 50, 60, 120, 340 and 480 min were also observed as the same manners. As depicted in Fig. S3A and B,† the recoveries of LTG and CBZ using methanol as desorption reagent were significantly higher than that of distilled water, but has no significant difference as compared with ethanol. When the desorption time was 60 min, the recovery of CBZ was the best. For LTG, when the desorption time was 4 h, the recovery was the highest, but has no significant difference with that of 60 min. Thus, methanol was selected as desorption reagent and the desorption time was set at 60 min in this work.

3.6. Reusability and stability

Reusability and stability are the important property of Dt-MMIPs.[26] To investigate the reusability, Dt-MMIPs which were used for CBZ and LTG rebinding were rinsed with 3 mL of methanol by shaking for 60 min and then dried under vacuum. The reclaimed Dt-MMIPs were used to extract CBZ and LTG from serum. Six adsorption–desorption cycles were carried out, and the extraction recovery of CBZ and LTG decreased slowly with an increase in cycle number and lost 12.5% and 7.8% after six cycles, respectively. This result may be attributed to the fact that the shape and distribution of the functional groups of imprinting sites were destroyed during repeated elution. The few losses in extraction recoveries indicate the good reusability of Dt-MMIPs. According to the experimental conditions of Dt-MMIPs used in the extraction of CBZ or LTG, the stability of Dt-MMIPs was observed by placing under room temperature or 4 °C (refrigerator) for 14 days. The RSD values of extraction recoveries of CBZ and LTG in serum for six adsorption–desorption cycles were used to evaluate the stability of Dt-MMIPs. The results showed that the RSD values of extraction recoveries of CBZ and LTG in serum were all less than 8.6%, which hinted that our prepared Dt-MMIPs were stable for 14 days under room temperature or 4 °C.

3.7. Application evaluation

The above results hinted that Dt-MMIPs possessed good absorption capacity and selectivity, however, it was still needed to be further validated and evaluated using biological sample due to its matrix complexity differed to *in vitro* samples. In this study, analytical performances of developed SPE based on Dt-MMIPs coupled with HPLC-UV was first validated from the aspects of selectivity, linearity, accuracy and precision, stability and extraction recovery by comparing with acetonitrile protein precipitation. Fig. 7 and 8 presented the chromatograms of QC samples after being treated with Dt-MMIPs or acetonitrile. We could find that whether detection at 285 nm (maximum absorption wavelength of CBZ, Fig. 7) or 307 nm (maximum absorption wavelength of LTG, Fig. 8), matrix interferences in Dt-MMIPs treatment were less than that of acetonitrile protein precipitation, and the peak shape of LTG detected at 307 nm was better. These results hinted that Dt-MMIPs possessed higher selectivity than acetonitrile protein precipitation. Table S1† showed the linearity, ranges and lower limit of quantification (LLOQ) of CBZ and LTG in QC samples treated with Dt-MMIPs or acetonitrile, and no obvious difference could be found between two kinds of different sample treatment methods. Intra-batch and inter-batch accuracy and precision were respectively shown in Tables S2 and S3.† Although obvious differences of intra-batch and inter-batch accuracy and precision at the low level of QC samples could be observed, however,

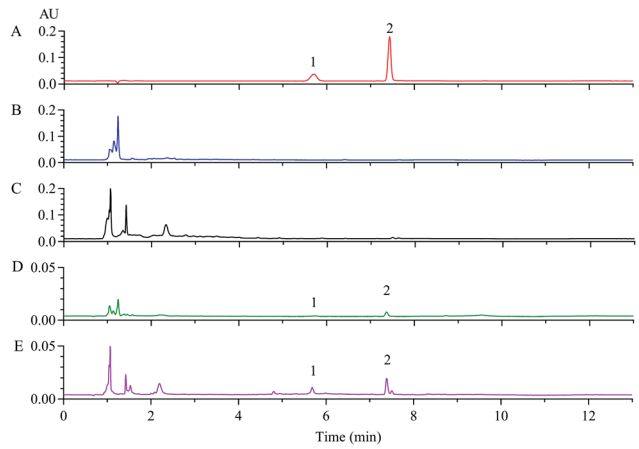

Fig. 7 The chromatograms of mixed standard solution of CBZ and LTG at the concentrations of 3 μg mL^{-1} (A), rat blank serum treated by acetonitrile protein precipitation (B) or dispersive SPE based on Dt-MMIPs (C), and rat blank serum spiked with CBZ and LTG at the concentrations of 3 μg mL^{-1} treated by acetonitrile protein precipitation (D) or dispersive SPE based on Dt-MMIPs (E) detected at 285 nm.

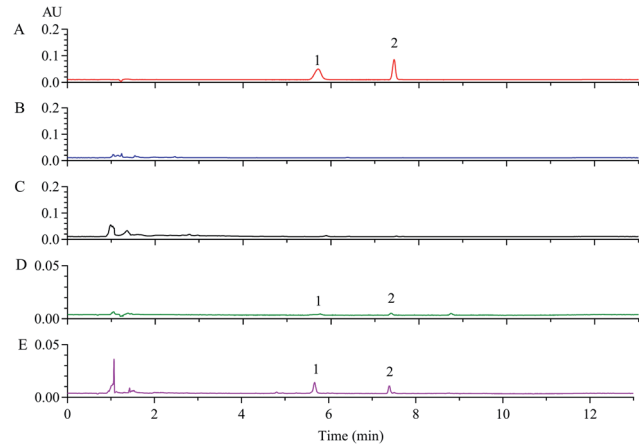

Fig. 8 The chromatograms of mixed standard solution of CBZ and LTG at the concentrations of 3 μg mL^{-1} (A), rat blank serum treated by acetonitrile protein precipitation (B) or dispersive SPE based on Dt-MMIPs (C), and rat blank serum spiked with CBZ and LTG at the concentrations of 3 μg mL^{-1} treated by acetonitrile protein precipitation (D) or dispersive SPE based on Dt-MMIPs (E) detected at 307 nm.

the values of accuracy and precision from two kinds of sample treatment methods were all meet the requirements of biological sample analysis. Table S4† gave the results of extraction recovery, and higher extraction recoveries in acetonitrile protein precipitation could be obtained, which might be attributed to the lower selectivity of acetonitrile. In general, the long-term freezing, short-term storage and freeze–thaw cycle stabilities of biological samples were not influenced obviously by different sample treatment methods. However, the supernatant stability of biological sample after treatment might be closely related to different sample prepared methods. Thus, in this study, the supernatant stability of rat serum after being Dt-MMIPs or acetonitrile was investigated by placing at 4 °C or 25 °C for 8 h, respectively. As shown in Table S5,† the supernatants of rat serum from two kinds of sample treatment were all stable under observed conditions, and no obvious difference could be obtained. Finally, the dispersive SPE based on Dt-MMIPs or acetonitrile protein precipitation coupled to HPLC-UV was further compared by analyzing 6 real rat sera after oral administration of CBZ or LTG at a single dosage of 10 mg kg^{-1}. Referring to the C_{max} of CBZ or LTG in the references, the sampling times were all set at 2 h.[27,28] As depicted in Table S6,† no obvious difference between two different sample treatment methods could be observed, however, the concentration of CBZ or LTG in rat serum treated by dispersive SPE based on Dt-MMIPs was higher than that of acetonitrile protein precipitation and more prone to the values of the references.[27,28]

4. Conclusions

In current study, a novel Dt-MMIPs using CBZ and LTG as the templates that could be simultaneously used to treat serum contained CBZ or LTG was first prepared. The maximum adsorption amount of the Dt-MMIPs towards CBZ or LTG was 249.5 μg g^{-1} and 647.9 μg g^{-1}, respectively, and the obtained Dt-MMIPs possessed a higher adsorption capacity and better specific recognition performance than MNIPs. The absorption behaviors of CBZ and LTG followed the pseudo-second-order kinetics equation well. Furthermore, the Dt-MMIPs possessed magnetic responsiveness and could be dispersed into solutions directly and separated quickly with an external magnet without SPE column packing. The selectivity and accuracy of developed magnetic dispersive SPE based on Dt-MMIPs approach was higher than conventional acetonitrile protein precipitation for the determination of CBZ or LTG in real rat serum samples. Therefore, the synthesized Dt-MMIPs might provide an alternative selectivity for the determination of CBZ or LTG in biological samples and thus possess a potential ability in the application of clinical TDM of CBZ and LTG.

Author contributions

Conceptualization, Dao-quan Tang; methodology, Ya-qin Wei, Lin-lin Zhao, and Yu-xin You; software, Ya-qin Wei and Lin-lin Zhao; validation, Lin-lin Zhao and Yu-xin You; investigation, Ya-qin Wei, Lin-lin Zhao, and Yu-xin You; resources, Xiao-xiao Zheng and Yan-lin Zhao; data curation, Ya-qin Wei and Lin-lin Zhao; writing-original draft preparation, Ya-qin Wei and Lin-lin Zhao; writing-review and editing, Dao-quan Tang; supervision, Yan Du and Dao-quan Tang; project administration, Yan Du and Yu-xin You. All authors have read and agreed to the published version of the article.

Conflicts of interest

The authors declare no competing financial interests.

Acknowledgements

This work is financially supported by the Natural Science Foundation of Jiangsu Province (No. BK20181147 and BE2019640).

References

1 M. L. Scheuer and T. A. Pedley, The evaluation and treatment of seizures, *N. Engl. J. Med.*, 1990, **323**, 1468–1474.
2 R. E. Pearce, G. R. Vakkalagadda and J. S. Leeder, Pathways of carbamazepine bioactivation *in vitro* I. Characterization of human cytochromes P450 responsible for the formation of 2- and 3-hydroxylated metabolites, *Drug Metab. Dispos.*, 2002, **30**, 1170–1179.
3 M. J. Leach, C. M. Marden and A. A. Miller, Pharmacological studies on lamotrigine, a novel antiepileptic drug II. Neurochemical studies on the mechanism of action, *Epilepsia*, 1986, **27**, 490–497.
4 C. J. Landmark, S. I. Johannessen and T. Tomson, Dosing strategies for antiepileptic drugs: from a standard dose for all to individualised treatment by implementation of therapeutic drug monitoring, *Epileptic Disord.*, 2016, **18**, 367–383.

5 J. M. Juenke, K. A. Miller, M. A. Ford, G. A. McMillin and K. L. Johnson-Davis, A comparison of two FDA approved lamotrigine immunoassays with ultra-high performance liquid chromatography tandem mass spectrometry, *Clin. Chim. Acta*, 2011, **412**, 1879–1882.

6 P. A. Datar, Quantitative bioanalytical and analytical method development of dibenzazepine derivative, carbamazepine: a review, *J. Pharm. Anal.*, 2015, **5**, 213–222.

7 S. Ghatol, V. Vithlani, S. Gurule, A. Khuroo, T. Monif and P. Partani, Liquid chromatography tandem mass spectrometry method for the estimation of lamotrigine in human plasma: application to a pharmacokinetic study, *J. Pharm. Anal.*, 2013, **3**, 75–83.

8 M. Shipkova, D. T. Petrova, A. E. Rosler, M. Orth, J. Engelmayer, E. Wieland, G. Brandhorst and M. Oellerich, Comparability and imprecision of 8 frequently used commercially available immunoassays for therapeutic drug monitoring, *Ther. Drug Monit.*, 2014, **36**, 433–441.

9 J. Taibon, R. Schmid, S. Lucha, S. Pongratz, K. Tarasov, C. Seger, C. Timm, R. Thiele, J. M. Herlan and U. Kobold, An LC-MS/MS based candidate reference method for the quantification of carbamazepine in human serum, *Clin. Chim. Acta*, 2017, **472**, 35–40.

10 E. K. Oh, E. Ban, J. S. Woo and C. K. Kim, Analysis of carbamazepine and its active metabolite, carbamazepine-10,11-epoxide, in human plasma using high-performance liquid chromatography, *Anal. Bioanal. Chem.*, 2006, **386**, 1931–1936.

11 K. K. Namdev, J. Dwivedi, D. C. Chilkoti and S. Sharma, A simple, rapid and stability indicating validated method for quantification of lamotrigine in human plasma and dry plasma spot using LC-ESI-MS/MS: application in clinical study, *J. Chromatogr. B: Anal. Technol. Biomed. Life Sci.*, 2018, **1072**, 362–369.

12 L. Zufía, A. Aldaz, N. Ibáñez and C. Viteri, LC method for the therapeutic drug monitoring of lamotrigine: evaluation of the assay performance and validation of its application in the routine area, *J. Pharm. Biomed. Anal.*, 2009, **49**, 547–553.

13 A. Ferreira, M. Rodrigues, P. Oliveira, J. Francisco, A. Fortuna, L. Rosado, P. Rosado, A. Falcão and G. Alves, Liquid chromatographic assay based on microextraction by packed sorbent for therapeutic drug monitoring of carbamazepine, lamotrigine, oxcarbazepine, phenobarbital, phenytoin and the active metabolites carbamazepine-10,11-epoxide and licarbazepine, *J. Chromatogr. B: Anal. Technol. Biomed. Life Sci.*, 2014, **971**, 20–29.

14 I. D. de Souza, D. S. Domingues and M. E. C. Queiroz, Hybrid silica monolith for microextraction by packed sorbent to determine drugs from plasma samples by liquid chromatography-tandem mass spectrometry, *Talanta*, 2015, **140**, 166–175.

15 M. Guo, L. Shao, Y. Du, Z. Qian, T. Huang and D. Tang, Microporous polymer based on the new compound "bi-(4-vinyl phenylquinoline) amide" for enrichment and quantitative determination of lamotrigine in rat and human serum, *Anal. Bioanal. Chem.*, 2019, **411**, 3353–3360.

16 M. Behbahani, S. Bagheri, M. M. Amini, H. Sadeghi Abandansari, H. Reza Moazami and A. Bagheri, Application of a magnetic molecularly imprinted polymer for the selective extraction and trace detection of lamotrigine in urine and plasma samples, *J. Sep. Sci.*, 2014, **37**, 1610–1616.

17 S. A. Mohajeri and S. A. Ebrahimi, Preparation and characterization of a lamotrigine imprinted polymer and its application for drug assay in human serum, *J. Sep. Sci.*, 2018, **31**, 3595–3602.

18 H. Kefayati, Y. Yamini, M. Shamsayei and S. Abdi, Molecularly imprinted polypyrrole@CuO nanocomposite as an in-tube solid-phase microextraction coating for selective extraction of carbamazepine from biological samples, *J. Pharm. Biomed. Anal.*, 2021, **204**, 114256.

19 R. Wang, Y. Cui, F. Hu, W. Liu, Q. Du, Y. Zhang, J. Zha, T. Huang, M. Fizir and H. He, Selective recognition and enrichment of carbamazepine in biological samples by magnetic imprinted polymer based on reversible addition-fragmentation chain transfer polymerization, *J. Chromatogr. A*, 2019, **1591**, 62–70.

20 F. Khalilian and S. Ahmadian, Molecularly imprinted polymer on a SiO_2-coated graphene oxide surface for the fast and selective dispersive solid-phase extraction of carbamazepine from biological samples, *J. Sep. Sci.*, 2016, **39**, 1500–1508.

21 G. Szekely, J. Bandarra, W. Heggie, F. C. Ferreira and B. Sellergren, Design, preparation and characterization of novel molecularly imprinted polymers for removal of potentially genotoxic 1,3-diisopropylurea from API solutions, *Sep. Purif. Technol.*, 2012, **86**, 190–198.

22 X. L. Wang, H. F. Yao, X. Y. Li, X. Wang, Y. P. Huang and Z. S. Liu, pH/temperature-sensitive hydrogel-based molecularly imprinted polymers (hydroMIPs) for drug delivery by frontal polymerization, *RSC Adv.*, 2016, **6**, 94038–94047.

23 M. Guo, L. Zhang, Y. Du, W. Du, D. Liu, C. Guo, Y. Pan and D. Tang, Enrichment and quantitative determination of 5-(hydroxymethyl)-2'-deoxycytidine, 5-(formyl)-2'-deoxycytidine, and 5-(carboxyl)-2'-deoxycytidine in human urine of breast cancer patients by magnetic hyper-cross-linked microporous polymers based on polyionic liquid, *Anal. Chem.*, 2018, **90**, 3906–3913.

24 S. C. Leeuwenburgh, I. D. Ana and J. A. Jansen, Sodium citrate as an effective dispersant for the synthesis of inorganic-organic composites with a nanodispersed mineral phase, *Acta Biomater.*, 2010, **6**, 836–844.

25 P. Kadhirvel, A. Combès, L. Bordron and V. Pichon, Development and application of water-compatible molecularly imprinted polymers for the selective extraction of carbamazepine from environmental waters, *Anal. Bioanal. Chem.*, 2019, **411**, 1525–1536.

26 J. Kupai, M. Razali, S. Buyuktiryaki, R. Kecili and G. Szekely, Long-term stability and reusability of molecularly imprinted polymers, *Polym. Chem.*, 2017, **8**, 666–673.

27 D. Singh and M. Asad, Effect of soybean administration on the pharmacokinetics of carbamazepine and omeprazole in rats, *Fundam. Clin. Pharmacol.*, 2010, **24**, 351–355.
28 S. Ventura, M. Rodrigues, S. Pousinho, A. Falcão and G. Alves, An easy-to-use liquid chromatography assay for the analysis of lamotrigine in rat plasma and brain samples using microextraction by packed sorbent: application to a pharmacokinetic study, *J. Chromatogr. B: Anal. Technol. Biomed. Life Sci.*, 2016, **1035**, 67–75.